

# TURBULENT FLAME PROPAGATION IN LARGE UNCONFINED H<sub>2</sub>/O<sub>2</sub>/N<sub>2</sub> CLOUDS

Daubech, J.<sup>1</sup>, Proust, C.<sup>1,2</sup> and Lecoq, G.<sup>1</sup>

<sup>1</sup> Institut de l'environnement industriel et des risques, PARC ALATA, BP2, Verneuil en Halatte, 60550, France, [jerome.daubech@ineris.fr](mailto:jerome.daubech@ineris.fr), [guillaume.lecoq@ineris.fr](mailto:guillaume.lecoq@ineris.fr)

<sup>2</sup> Université technologique de Compiègne, Centre Pierre Guillaumat, TIMR, bat E-D, Compiègne, 60200, France, [christophe.proust@utc.fr](mailto:christophe.proust@utc.fr)

## ABSTRACT

Turbulence is a key aspect in hydrogen explosions. Unfortunately, only limited experimental data is available and the current understanding of flame turbulence interactions is too limited to permit safe predictions. New experimental data are presented in which the flame trajectory and pressure history are interpreted for unconfined explosions of H<sub>2</sub>/O<sub>2</sub>/N<sub>2</sub> clouds of 7 m<sup>3</sup>. The intensity of the turbulence is varied between 0 and 5 m/s and the integral scale of the turbulence is on the order of 10 cm which is at least an order of magnitude larger than lab scale.

## 1.0 INTRODUCTION

The turbulent flame velocity is the key aspect to evaluate the explosion consequences in unconfined hydrogen deflagration. The regime of turbulent combustion is the result of a strong interaction between a compressible turbulent flow, the chemical processes of combustion, the mass and energy transfer and probably flame instabilities. Because of the degree on complexity, the predictability of existing models is limited. In industrial safety, the length scales and the intensities of turbulent flows are not sufficient such that the flame front is totally disrupted as compared to a laminar situation[1]. The turbulent flame is rather described as a laminar flame convected and stretched by the turbulent vortices. The issue is to be able to describe this interaction.

The intensity of flow velocity fluctuations  $u'$  and the characteristic length of vortices  $L_t$  seem enough to describe conveniently the turbulent flow field [2]. The laminar flame can be well described by the laminar burning velocity  $S_{lad}$ . But, this fundamental parameter is not sufficient to cover all the flame dynamic like the interaction with turbulence or the combustion instabilities. Several approaches had been discussed by authors.

According Williams [3], the typology of turbulent flame in an industrial cloud is a "laminar wrinkled" flame. A few authors like Gülder or Abdel-Gayed [4,5] proposed an approach based on a dimensional analysis, but it is not completely coherent and don't take into account some important aspects as the effects of flame instabilities. Others works supposed that the burn-up of a turbulent flame can directly described by a well knowledge of flame surface. This surface could be deduced from the fractal theory [6, 7]. But this situation supposed that the flame are considered completely passive, that is to say if  $u' \gg S_{lad}$ . Nevertheless, Smallwood [8] or Yoshida [9] showed that it kind of flame cannot be described by the fractal theory of flame.

Another way could be to consider the industrial turbulent flame as a laminar flame slightly disturbed. The theories of asymptotic development [10, 11] could be a possibility to analyze the flame structure.

This paper tries to present new experimental data on flame propagation in turbulent cloud and to give a physical interpretation of flame behavior.

New experiments were realized during the BARPPRO French R&D project dedicated to the protection of industrial facilities against the blast of explosions. A specific device was developed to produce calibrated "N" waves issued from fast deflagrations. This paper presents the device and the main results of overpressure and flame velocities for quiescent and turbulent and hydrogen-oxygen-air mixtures in 7 m<sup>3</sup> cloud. A discussion of these results is also proposed for flame behavior.

## 2.0 EXPERIMENTAL CONDITIONS

The experimental set-up is composed by:

- A test platform supporting a 3 m diameter hemisphere covered with a transparent plastic sheet,
- A device for gas dispersion,
- Pressure, concentration measurement and fast camera.

### 2.1 Test platform

The test platform (Fig.1) is a metallic structure in 3.5 cm thick IPN structure covered with a 5 mm metal plate. It is equipped with 8 spikes on which 8 flexible plastic tubes are inserted to form a sort of hemispheric frame having a radius of 1.5 m. The free ends of the plastic tubes are connected together by metal



Figure 1. Test platform

This structure covered with a 150  $\mu\text{m}$  transparent plastic sheet (Fig. 1). This sheet is maintained to the structure thanks to an elastic cord retained by an electromagnet. This elastic cord presses the plastic sheet against aluminium profiles fixed on the platform to ensure a good sealing. The elastic cord is released 300 to 800 ms before the ignition.

### 2.2 Mixture preparation

The gas is injected under a pressure of 5 bar in the hemisphere using 4 jetflows (figure 3).



Figure 3. Jetflow

Four jetflows are settled in the hemisphere face to face in pairs. The end of the gas ejection cone is placed 90 cm from the center of the platform. The arrival of the gases in the jetflows is through a system of an inch pipes under the metal plate (Fig.5). The flow created in the hemisphere provides sufficient mixing to obtain a homogeneous mixture. Jetflows use the coanda effect where a jet of gas hugs the side of a curved surface to create air motion. Using a small amount of compressed air as their

power source, jetflows entrain and pull in large volumes of surrounding air to produce volume, velocity outlet flows (Fig.4).

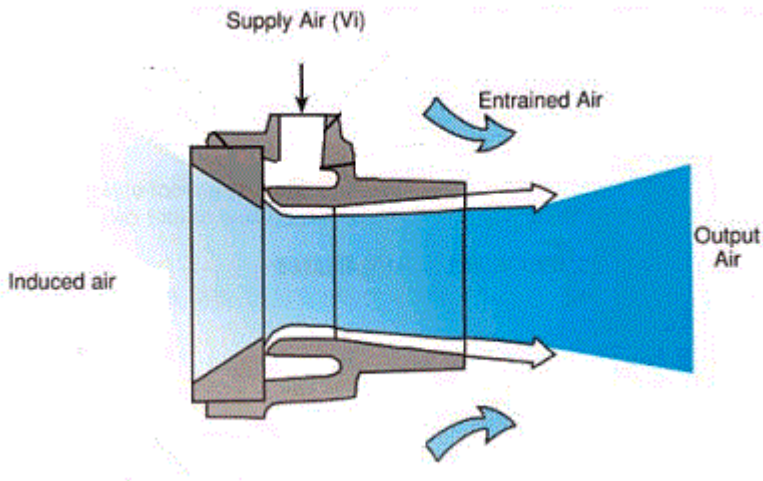


Figure 4. Principle of jetflow

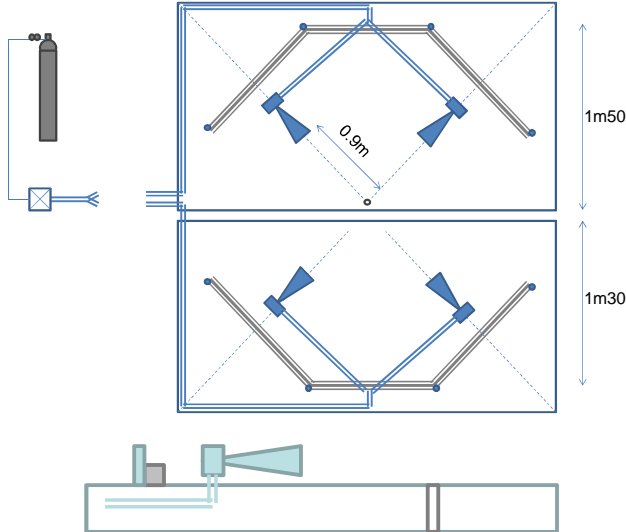


Figure 5. Gas dispersion device

The jetflows are also used to generate the turbulence.

**2.3 Instrumentation**

The concentration and homogeneity of the mixture are controlled in two points using two oxygen analyzers. The two sampling points are located at 0.1 m and 1.4 m from the test platform.

The ignition is obtained using a pyrotechnical match (60 J) installed at the centre of the hemisphere on the floor.

Two pressure Kistler 0-10 bar (accuracy :  $\pm 0.1$  % full scale) gauges are used to measure overpressures. One is located at the center of the hemisphere to measure the overpressure in the burnt gases and the second is located at 10 m from the center of hemisphere to measure the pressure wave in the near field.

The visualization of the explosion is realized using a PHOTRON fast video camera.

## 2.4 Flammable mixtures

The flammable mixture used contain hydrogen, oxygen and nitrogen (Tab.1)

Table 1. Characteristics of the mixture

	Mixture 1	Mixture 2
% H2	40	45
% O2	20	22.5
% N2	40	32.5
Laminar flame speed $S_{lad}$ (m/s)	3.5	4.2
Expansion ratio $\alpha$	7.8	8

The burning properties of the mixture were determined using a semi-experimental method [11]. First, the adiabatic temperature of combustion and the expansion ratio were estimated using a thermodynamic code similar to CEA (NASA code). Then, experimental results for the burning

velocities were interpolated using the theoretical law 
$$S_{lad} = \left[ \frac{2 \cdot \lambda \cdot Le \cdot Z' \cdot R \cdot T_f^2 \cdot \exp\left(\frac{-E_a}{RT_f}\right)}{\rho_0 \cdot E_a \cdot c_p \cdot (T_f - T_0)} \right]^{\frac{1}{2}}$$
 which links  $S_{lad}$

and flame temperature.

where  $T_f$  is the adiabatic flame temperature,  $E_a$  is the activation energy,  $Le$  is the Lewis number,  $Z$  is the Zeldovitch number,  $C_p$  is the specific heat.

Thus, the evolution of  $S_{lad}$  as a function of adiabatic flame temperature (Fig.6) is built noticing that the variations of flame velocity are largely determined by the evolution of combustion temperature (hypothesis of “high activation energy”) through  $\exp(-E_a/RT_{ad})$ . This graph is confronted with experimental data relevant to stoichiometric H2-O2 mixtures diluted with nitrogen [12, 13] at Fig. 5.

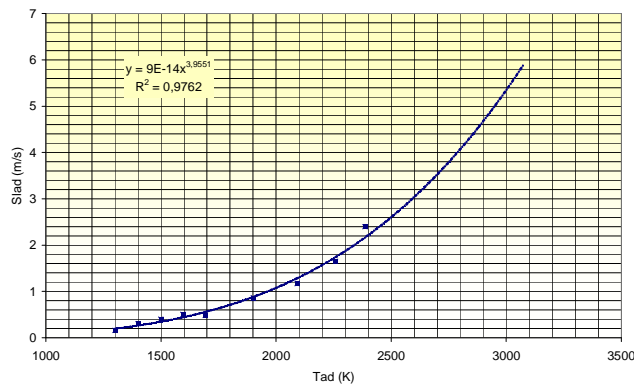


Figure 6. Laminar flame speed vs adiabatic combustion temperature for stoichiometric H2-O2 mixture diluted with N2

## 2.5 Characterization of turbulence

An earlier version of the test platform used a 1500 m<sup>3</sup>/h fan sucking the mixture by a hole and reinjecting it by two holes creating a turbulent flow in the hemisphere (Fig.7).

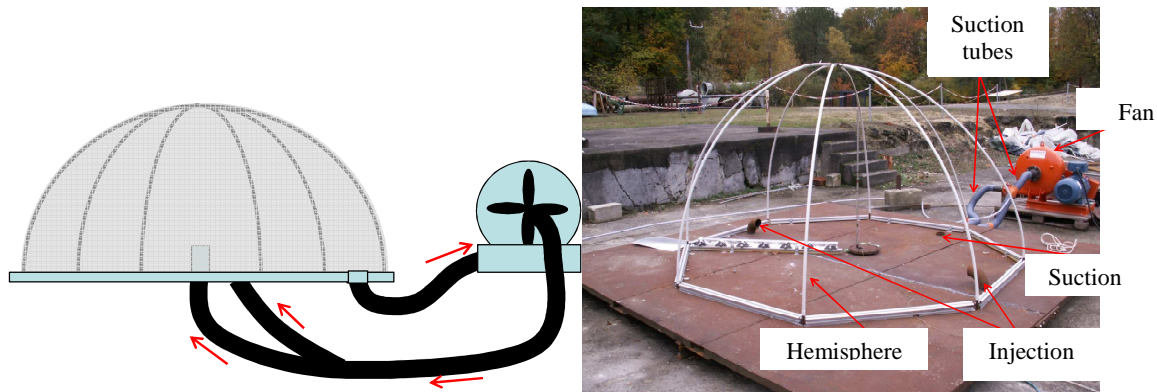


Figure 7. Earlier version of the test platform

Measurements of turbulence were done in this hemisphere with 3 Pitot probes [14] linked to differential pressure sensors (Fig. 8) in 3 locations.



Figure 8. Pitot probes

This probes measures the flow field and the turbulent motion of the atmosphere in the dome. An important work of comparison between Pitot probe and hot wire anemometer was done and will be published shortly. For this experimental configuration, they measure a turbulent intensity of 5 m/s. The characteristic length scale is determined by calculation of temporal autocorrelation and is equal to 0,15 m. A simulation of this flow field was done using PIMPLEFOAM solver of OPENFOAM (Fig.9)

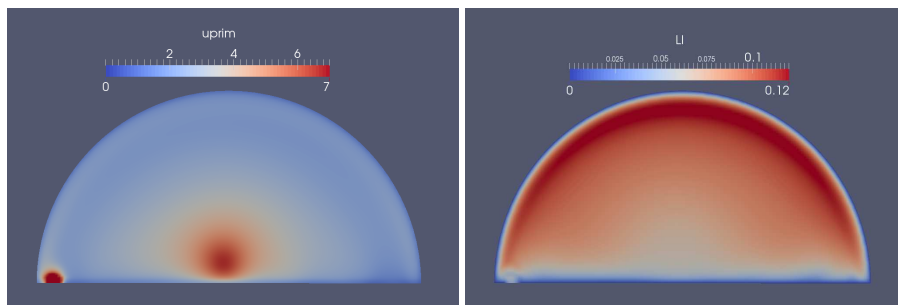


Figure 9. PIMPLEFOAM simulation for fan configuration –  $u'$  and  $L_t$

The simulations are in a reasonable agreement with the experimental measurements. So, the PIMPLEFOAM solver [15] was used to calibrate turbulence in jetflow configuration in which measurement of turbulence were not done. Fig. 9 presents the results obtained for turbulent intensity

$u'$  and length scale  $L_t$ . The mean length scale  $L_t$  is around 0.16 m and the mean turbulent intensity is around 1.5 m/s (Fig.10).

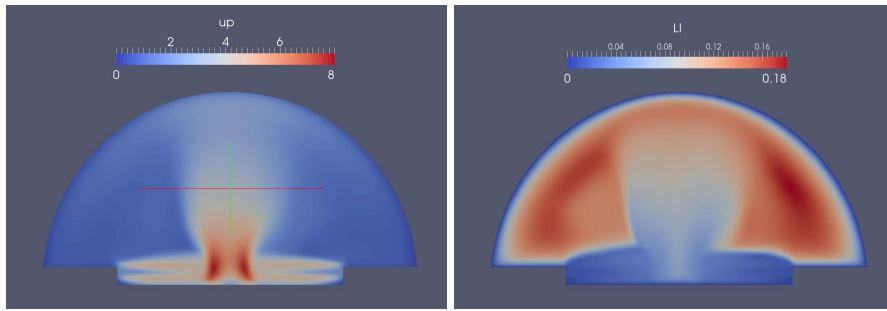


Figure 10. PIMPLEFOAM simulation for jetflow configuration –  $u'$  and  $L_t$

### 3.0 ANALYSIS OF TYPICAL RESULTS

The explosion test of quiescent mixtures is analysed in more details below.

#### 3.1 Pressure signals

The pressure signals are shown on Fig.11 and some excerpts from the film on Fig.12. The typical burnt gas overpressure and overpressure at 10 m are presented for mixture 1. The maximum overpressure in the burnt gas is obtained at 0.036 s. Fig 7 presents the typical evolution of flame during the deflagration at different times. The plastic sheet begins to move at 0.02 s after ignition.

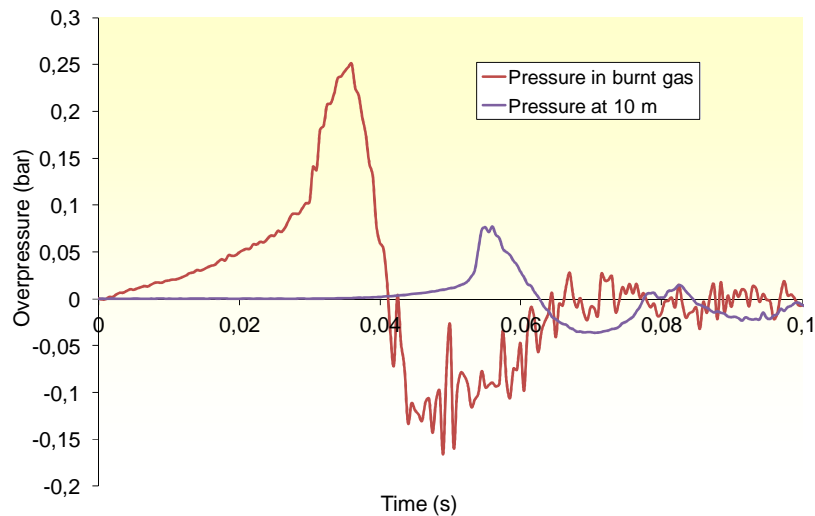


Figure 11. Burnt gas overpressure and overpressure at 10 m – Quiescent mixture (mixture 1 : 40 % H<sub>2</sub>, 20 % O<sub>2</sub>, 40 % N<sub>2</sub>)

A specific treatment was used to extract the flame trajectory and velocity. The white line on the picture defines the flame shape resulting from the treatment. The time between two pictures is 2.5 ms.



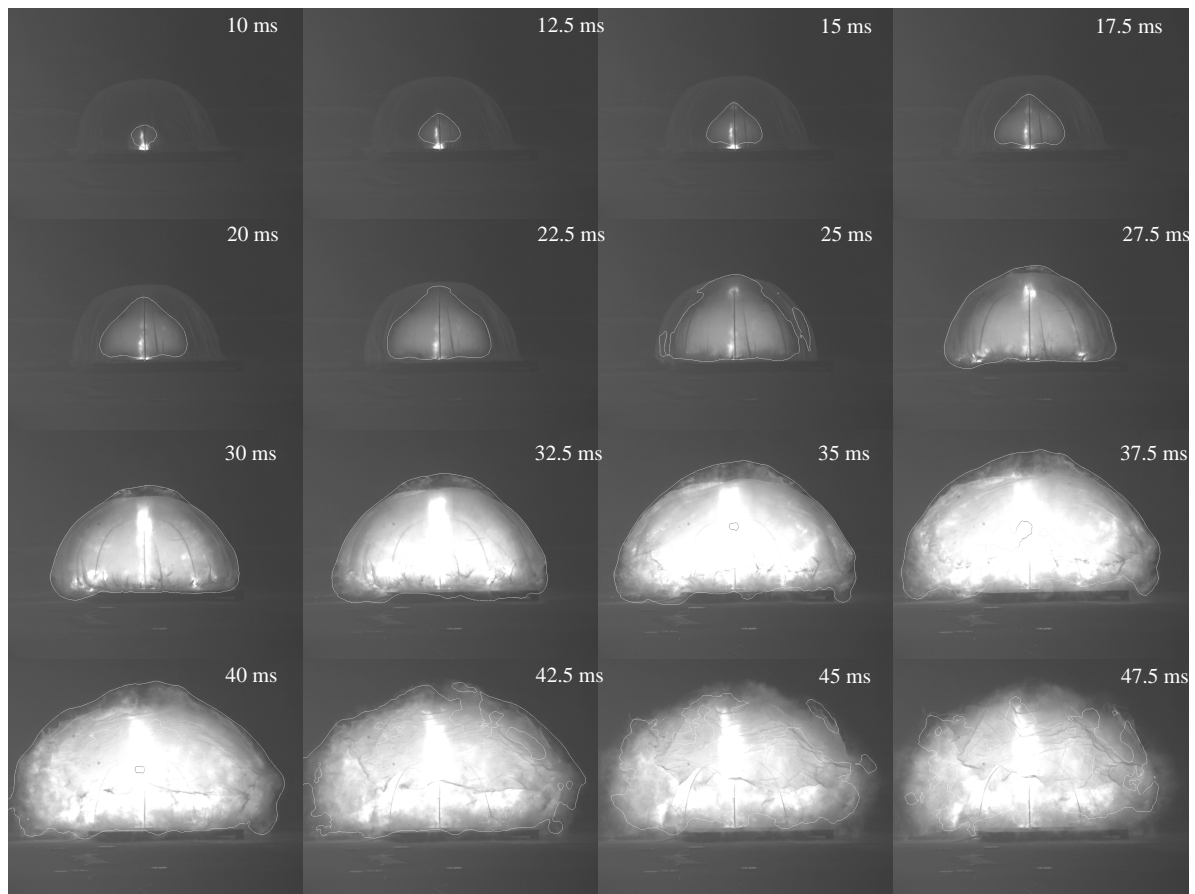


Figure 12. Evolution of the flame at different times - The time between two pictures is 2.5 ms

The typical burnt gas overpressure and overpressure at 10 m are presented for mixture 2 on Fig.13. The maximum overpressure in the burnt gas is obtained at 0.025 s. The plastic sheet begins to move at 0.012 s after ignition.

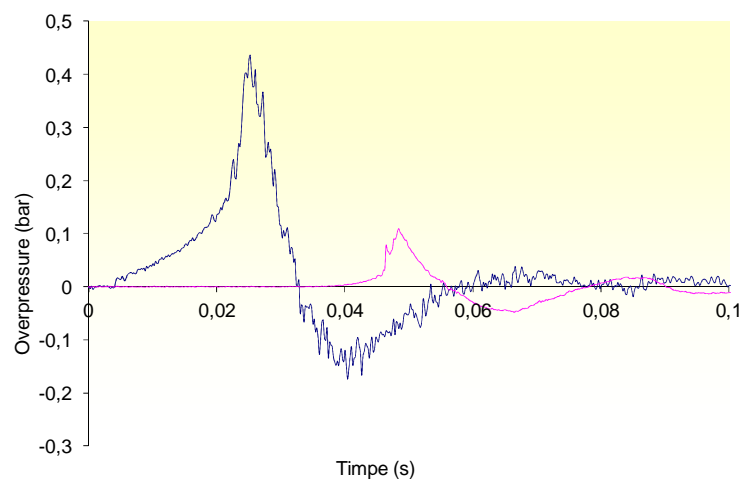


Figure 13. Burnt gas overpressure and overpressure at 10 m – Quiescent mixture (mixture 2 : 45 % H<sub>2</sub>, 22.5 % O<sub>2</sub>, 32.5 % N<sub>2</sub>)

### 3.2 Flame trajectory and speed

The Fig. 14 presents the flame trajectory and the flame propagation velocity deduced from the high speed camera for mixture 1.

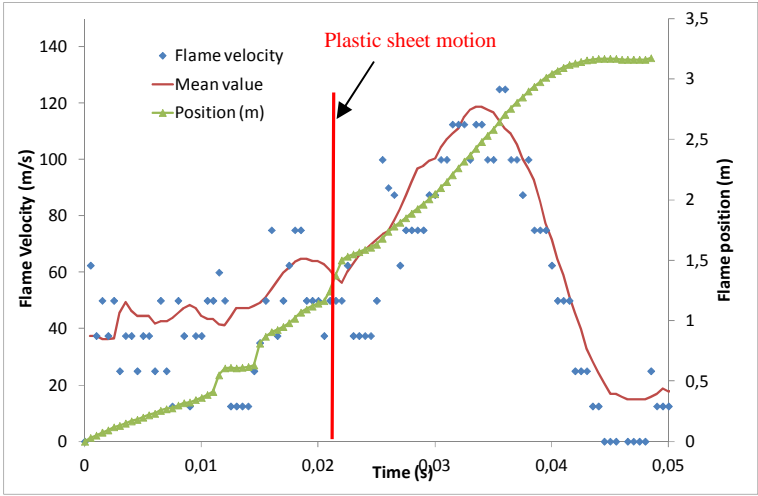


Figure 14. Flame trajectory and flame propagation velocity – Mixture 1

The flame trajectory (Fig.15) presents some discontinuities linked to the automatic treatment of high speed video. But, it gives a good idea of evolution of flame trajectory and velocity of flame.

The evolution of velocity contains two distinct parts. The first part of the evolution is quite constant around 45 m/s. It's consistent with the evolution of the overpressure in the burn gas for which the pressure rise is linear until 0.022 s. After that, the velocity increases by 45 to 115 m/s. This increase is also present on the overpressure signal with an exponential evolution to reach 250 mbar at 0.036 s.

The beginning of this strong acceleration seems to be linked to the motion of the plastic sheet. This motion creates an accelerating motion of the flame due to, perhaps, a creation of zone of turbulent/shear flow between the the flame front and the plastic envelope.

The Fig. 15 presents the flame trajectory and the flame propagation velocity deduced from the high speed camera for mixture 2.

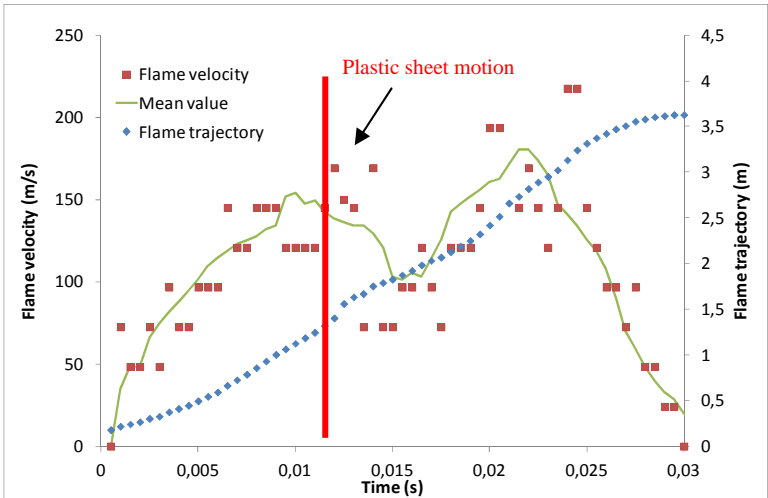


Figure 15. Flame trajectory and flame propagation velocity – Mixture 1

The evolution of velocity consists again in two distinct parts. The first part of the evolution is a constant evolution to reach a mean value around 140 mbar. After that, the velocity decreases by 140 to 100 m/s and increases to reach it maximum value around 200 m/s at 0.025 s.

#### 4.0 COMPARISON BETWEEN QUIESCENT AND TURBULENT MIXTURES

This section present the comparison between the quiescent and turbulent stoichiometric H<sub>2</sub>-O<sub>2</sub> mixture diluted with N<sub>2</sub>. The turbulence is obtained using the 4 jetflows during the injection of gas.

Fig. 16 presents a superposition of the burnt gas overpressures for the quiescent and the turbulent mixtures. As for the quiescent mixture, the pressure signal has two parts. The analysis of high speed movie reveals that the strong pressure rise-up is also linked to the motion of the plastic sheet occurring around 0.016 s. If we focus on the end of flame propagation and, we compare the maximum flame speed obtained at the end of propagation (Fig. 17), we noticed that the maximum velocity for turbulent mixture is around 100 m/s whereas it's around 115 m/s for the quiescent mixture. It explains the difference between the maximum overpressures obtained at the end of propagation.

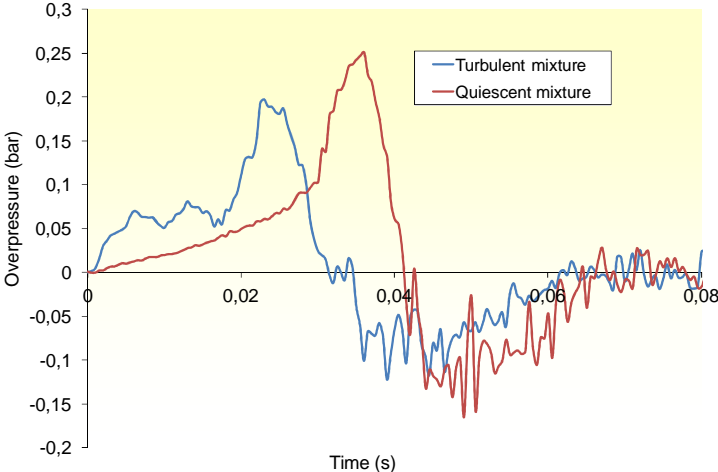


Figure 16. Burnt gas overpressures for the quiescent and the turbulent mixtures

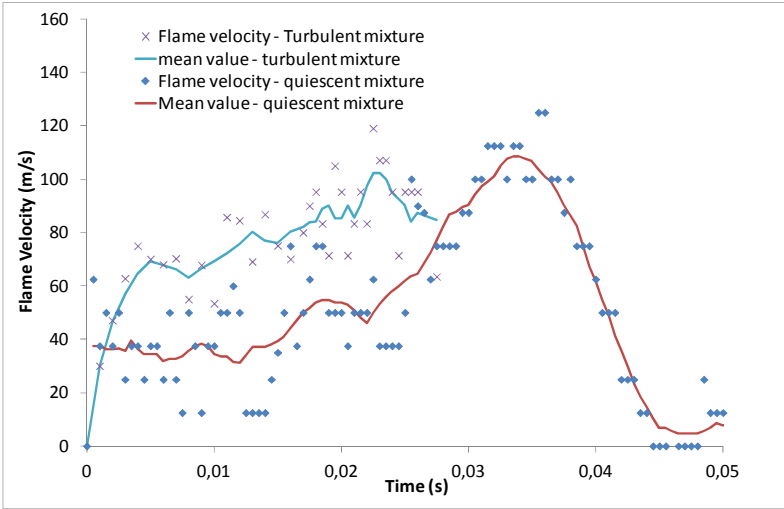


Figure 17. Flame velocities for the quiescent and the turbulent mixtures

Focus on the first part of flame propagation before the motion of plastic sheet. Before 16 ms, the flame propagates at 85 m/s (average). This velocity is 1.5 times higher than velocity in the quiescent mixture.

## 5.0 DISCUSSION

### 5.1 Plastic sheet effect

What is the influence of the motion of the plastic film on pressure wave generation? Thanks to the model of acoustic source [16], a reconstitution of 10 m pressure signal was done from the flame velocity deduced from high speed camera and from the inside overpressures (Fig.18). This latter speed integrates theoretically the influence of the plastic film motion. All the data are reasonable collapsed together suggesting a negligible influence of the envelope on the pressure wave generation and transmission. However, for quiescent or turbulent mixtures, a strong acceleration was observed when the plastic began to move directly observable on pressure signal. An analysis of high speed video shows that increase of flame speed is global (if the speed of several point of plastic sheet are followed, each point registered the same increase of velocity). This acceleration of flame could be linked to the appearance of an important shear zone under the plastic sheet. This zone could be responsible for a huge increase of combustion rate by a wrinkling of flame front. The CFD simulation may be a help to investigate this further in the future.

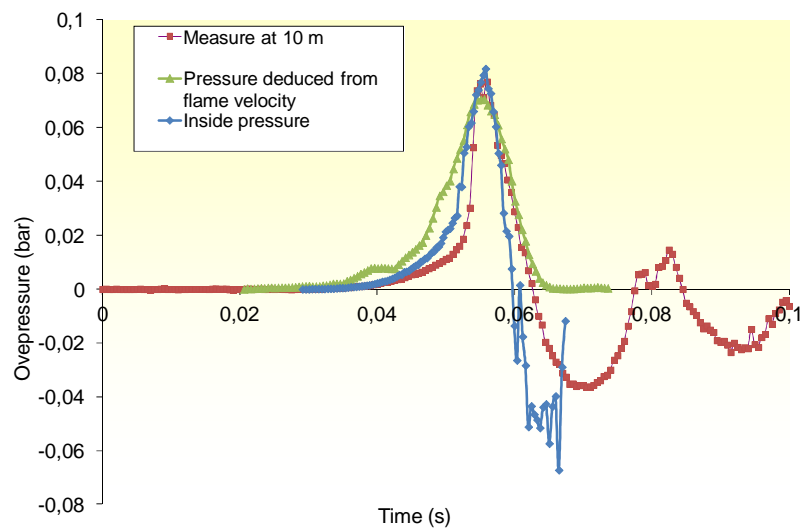


Figure 18. Reconstitution of 10 m pressure signal from flame velocity and inside overpressure

### 5.2 Hydrodynamic instability effect

Focuses the first part of flame propagation for quiescent stoichiometric H<sub>2</sub>-O<sub>2</sub> mixtures diluted by N<sub>2</sub>.

The properties of reactivity of each mixture are presented in paragraph 2.4 and a summary of the main results is given in Tab. 2

Table 2. Theoretical and experimental flame velocity (initially quiescent mixtures)

Mixture	Expansion ratio $\alpha$	Laminar flame speed $S_{lad}$ (m/s)	$\alpha \cdot S_{lad}$ (m/s)	Measured flame propagation (m/s)	Ratio
1	7.5	3.5	26	50	~2
2	8	4.2	34	140	~4

For the two mixtures, a coefficient of 2 to 4 exists between the theoretical and measured flame speed. This observation is consistent with previous works [17] which suggests that hydrodynamic instabilities could be responsible for self acceleration of flame (as for mixture 2 explosion) even if the mixture is

quiescent and far from any walls. These works confirmed also the increase of combustion rate and showed that increase factor of combustion velocity under hydrodynamic instabilities effect is around 3 and could depends on the size of the cloud (Fig. 19)

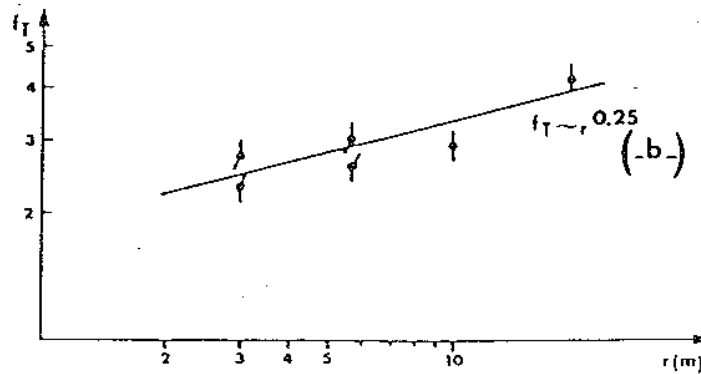


Figure 19. Flame velocity vs distance, spherical explosion of stoichiometric hydrogen-air mixtures [18]

### 5.3 Turbulence effect

The comparison between quiescent and turbulent mixture for mixture 1 reveals the real impact of turbulence in flame propagation. For the same reactivity, the turbulent flame is ~1.5 times faster than “quiescent” flame.

The maximum value of turbulent flame propagation speed is around 85 m/s, which represent a turbulent flame speed around 11 m/s.

Winiger [19] performed recently an intercomparison between the different correlations to calculate turbulent flame speed. This study shows that correlations of Bray ( $\frac{S_T}{S_L} = 0.875 \cdot K^{-0.392} \cdot \left(\frac{u'}{S_L}\right)$ , [20]), Shy ( $\frac{S_T}{S_L} = 1 + 0.05 \left(\frac{u'}{S_L}\right)^{0.39} \left(\frac{L_t}{\eta}\right)^{0.61}$ , [21]), and Gülder ( $\frac{S_T}{S_L} = 1 + 0.7 \left(\frac{u'}{S_L}\right)^{0.75} \left(\frac{L_t}{\eta}\right)^{0.25}$ , [22]) performed reasonably against experimental results (where  $u'$  - turbulent intensity,  $L_t$  - turbulent length scale,  $\eta$  - flame thickness,  $K$  - Karlovitz number).

These correlations are confronted to our experimental results in Tab. 3

Table 3. Comparison between Bray, Shy and Gülder correlations and experiment

Experiment	Bray	Shy	Gülder
11	25	33	14

Gülder correlation gives the best result and confirms the past INERIS choice to estimate the flame turbulent velocity.

### REFERENCES

1. MOUILLEAU Y., RUFFIN E. (1998), “Code de calcul des explosions dans les jets turbulents de gaz inflammables : synthèse des travaux de recherche et de validation”, rapport INERIS, ref INERIS EMA - YMo-ERu/YMo-98-16FA26

2. HINZE J.O. (1975), " Turbulence ", 2nd edition, Mc Graw-Hill company, New-York, ISBN 0-07-029037-7.
3. WILLIAMS F.A. (1985), " Combustion theory : 2nd edition ", Benjamin/Cummings publishing company Inc., Amsterdam, ISBN 0-8053-9801-5.
4. GÜLDER Ö.L. (1990), " Turbulent premixed flame propagation models for different combustion regimes ", Comptes-rendus du 22nd Symp (Int.) on Combustion
5. ABDEL-GAYED R.G., BRADLEY D., McMAHON M. (1978), " Turbulent flame propagation in premixed gases : theory and experiments ", Comptes-rendus du 17th Symp. (Int.) on Combustion
6. GOULDIN F.C. (1987), " An application of fractals to modelling of premixed turbulent flames ", Comb. and Flame, vol. 68, pp. 249-266.
7. PETERS N. (1986), " Laminar flamelet concepts in turbulent combustion, Comptes-rendus du 21st symp. (Int.) on Combustion, pp. 1231-1250.
8. SMALLWOOD G.J., GÜLDER Ö. L., SNELLING R.M., DESCHAMPS B., GÖKALP I. (1995), " Characterisation of flame front surfaces in turbulent premixed methane/air combustion ", Comb. and Flame, vol. 101, pp. 461-470
9. YOSHIDA A., ANDO Y., YANAGISAWA T., TSUJI H. (1994), " Fractal behaviour of wrinkled laminar flame ", Comb. Sci. and Tech., vol. 96, pp. 121-134
10. JOULIN G., CAMBRAY P. (1992), " On a tentative approximate evolution equation for markedly wrinkled premixed flames ", Comb. Sci. and Tech., vol. 81, pp. 243-256
11. DAUBECH J, (2008), Contribution à l'étude de l'effet de l'hétérogénéité d'un prémélange gazeux sur la propagation d'une flamme dans un tube clos, thèse de doctorat, Université d'Orléans
12. RITTLER D.L., 1953, "Activation energies of global reaction in laminar flame propagation", mémoire de thèse, California Institute of Technology
13. QIAO L., KIM C.H., FAETH G.M., 2005, "Suppression effects of diluents on laminar premixed hydrogen, oxygen, nitrogen flames", Comb. and Flame, vol 143, pp 79 - 96
14. MCCAFFREYB.J.; HESKESTAD.G, (1976) Robust Bidirectional Low-Velocity Probe for Flame and Fire Application
15. OpenFOAM Team, 2014. The OpenFOAM Foundation. <http://www.openfoam.org>
16. LEYER J.C. (1982), " Effets de pression engendrés par l'explosion dans l'atmosphère de mélanges gazeux d'hydrocarbures et d'air ", Revue Générale de Thermique, vol. 243, pp. 193-208
17. BRADLEY B., CRESSWELL T.M., PUTTOCK J.S., (2001): Flame acceleration due to flame-induced instabilities in large scale explosions, Comb and Flame, vol. 124, pp 551-559
18. DRENCKHAHN W., KOCH C., (1985): Transition from slow deflagration to detonation, Seminar on the results of the European Committees – Indirect Action Research Program on Safety of Thermal Water Reactors, Bruxelles, octobre 1985
19. WINIGER M, 2015, "Explosion – Caractérisation et vitesse de propagation de flamme dans un mélange turbulent", rapport de stage Université Technologique de Compiègne
20. BRAY KNC, (1990). ' Studies of turbulent burning velocities'. Proc R Soc Lond A 1990;431:315–35
21. SHY SS, LIN WJ, PENG KZ. (2000): "High intensity turbulent premixed combustion: general correlations of turbulent burning velocities in a new cruciform burner". Proc Combust Inst 2000;28:561–8
22. GÜLDER Ö.L. (1990), " Turbulent premixed flame propagation models for different combustion regimes ", Comptes-rendus du 22nd Symp (Int.) on Combustion